



Short communication

## Electrochemical behaviour of Heusler alloy $\text{Co}_2\text{MnSi}$ for secondary lithium batteries

Jun H. Park<sup>a</sup>, Dae H. Jeong<sup>a</sup>, Sang M. Cha<sup>a</sup>, Yang-Kook Sun<sup>b</sup>, Chong S. Yoon<sup>a,\*</sup><sup>a</sup> Department of Materials Science and Engineering, Hanyang University, Seoul 133-791, Republic of Korea<sup>b</sup> Department of Chemical Engineering, Hanyang University, Seoul 133-791, Republic of Korea

## ARTICLE INFO

## Article history:

Received 1 September 2008

Received in revised form 30 October 2008

Accepted 10 November 2008

Available online 3 December 2008

## Keywords:

Lithium-ion battery

Heusler alloy

Intermetallic compound

Negative electrode

Discharge capacity

Structural changes

## ABSTRACT

Electrochemical lithiation of  $\text{Co}_2\text{MnSi}$  with a Heusler structure is investigated as a candidate negative electrode (anode) material for secondary lithium batteries. The electrode maintains a reversible discharge capacity of  $112 \text{ mAh g}^{-1}$  for 50 cycles when cycled between 0.01 and 3 V. It is proposed that the lithiation mechanism consists of two steps.  $\text{Co}_2\text{MnSi}$  transforms to Heusler-type  $\text{Li}_2\text{MnSi}$  during the first charge cycle and subsequent charge–discharge cycles involve the formation of a solid solution in  $\text{Li}_x\text{MnSi}$ . The latter compound maintains its structural integrity throughout cycling to provide steady cycling behaviour. Magnetic measurements are also employed to substantiate further the structural changes during electrochemical cycling.

© 2008 Elsevier B.V. All rights reserved.

### 1. Introduction

Graphitic materials have been widely used as negative electrodes (anodes) for secondary lithium batteries. In spite of their success, graphitic anodes still suffer serious problems that include electrolyte decomposition and subsequent structural damage, which lead to irreversible capacity loss [1]. In order to meet the ever-increasing demand for lithium batteries with higher energy density ( $\text{Wh l}^{-1}$ ), alternative anode materials have been actively sought. Several materials, such as Sn-based alloys and compounds [2–8], and Si alloys and their composites [9–14], have been reported as possible alternatives. Despite the huge capacity (maximum of  $4200 \text{ mAh g}^{-1}$  for Si) obtainable from some of these materials, capacity loss originating from the large volume expansion during lithiation is the main limitation to their use as anode materials. To minimize the volume expansion, these materials have been introduced with promising success in the form of nanoparticles and nanowires [15–18]. Nevertheless, technologies required to scale up the synthesis of these nano-materials to an industrial level have not yet been developed. Transition metal oxides have also been shown to provide stable cycling behaviour as negative electrodes through electrochemically induced phase transformation during lithiation [19–21].

This paper examines a new class of material based on a ternary transition metal intermetallic system – Heusler alloys – as a potential electrode material for Li ion batteries. Recently, it was shown that  $\text{Li}_2\text{CuSb}$  with a Heusler structure was formed during Li-intercalation of  $\text{Cu}_2\text{Sb}$  [22], whereas  $\text{CoMnSb}$  with a half-Heusler-type structure exhibited a stable discharge capacity of  $220 \text{ mAh g}^{-1}$  through formation of lithiated  $\text{Li}_2\text{CoSb}$  phase during the first charge cycle [23]. It is supposed that  $\text{Co}_2\text{MnSi}$ , one of the representative Heusler alloys, would also maintain its structural integrity during Li uptake/removal.  $\text{Co}_2\text{MnSi}$  has a face-centered cubic (fcc) structure (space group  $F\bar{4}3m$ ) with a density of  $6.9 \text{ g cm}^{-3}$ , which is nearly twice the density of carbon. The high density of the material would provide a high energy density if  $\text{Co}_2\text{MnSi}$  were able to generate a reasonable level of discharge capacity. In this study, it is demonstrated that  $\text{Co}_2\text{MnSi}$  can maintain steady electrochemical cycling and its electrochemical behaviour is correlated to the changes in microstructure of the electrode as well as its magnetic properties.

### 2. Experimental

A  $\text{Co}_2\text{MnSi}$  ingot was produced by arc-melting a stoichiometric mixture of Co, Mn and Si powders. The initial structure and the composition of the ingot were verified by means of X-ray diffraction (XRD) and energy-dispersive X-ray spectroscopy (EDS). The  $\text{Co}_2\text{MnSi}$  ingot was ground in a high-speed ball mill using ethanol to prevent oxidation of the powder. The final particle size was 1–5  $\mu\text{m}$ .

\* Corresponding author. Tel.: +82 2 2220 0384; fax: +82 2 2220 1838.  
E-mail address: [csyoon@hanyang.ac.kr](mailto:csyoon@hanyang.ac.kr) (C.S. Yoon).

The electrochemical cycling was performed using a CR2032 coin-type cell. The anode consisted of 20 mg of accurately weighed active material and 12 mg of conductive binder (teflonized acetylene black). The material was pressed on to a copper mesh (1.6 cm in diameter) under a pressure of  $300 \text{ kg cm}^{-2}$  and dried at  $110^\circ\text{C}$  for 5 h. The test cell comprised the  $\text{Co}_2\text{MnSi}$  electrode with a lithium metal foil as the anode (Honjo Chemical Co.) that were separated by a porous polypropylene film (Celgard 3401). The electrolyte was 1 M  $\text{LiPF}_6$  in ethylene carbonate/dimethyl carbonate (1:1 by volume). The charge/discharge current density was maintained at  $0.2 \text{ mA cm}^{-2}$  with cut-off voltages of 0.01–3 V. To investigate the structural changes of the anode material after cycling, the tested cell was opened and rinsed with acetonitrile to remove the remaining  $\text{LiPF}_6$  salt. X-ray diffraction (Rigaku, Japan) using  $\text{CuK}\alpha$  radiation was used to characterize the microstructure of the powder at various stages of electrochemical cycling. A vibrating sample magnetometer was also employed to probe the magnetic properties of the cycled electrode.

### 3. Results and discussion

Fig. 1(a) shows typical charge–discharge curves of  $\text{Co}_2\text{MnSi}$  cycled at a current density of  $0.2 \text{ mA cm}^{-2}$ . The charge curve

indicates that 3.9 moles of Li are inserted into the  $\text{Co}_2\text{MnSi}$  electrode during the first cycle. The initial irreversible capacity loss ( $20 \text{ mAh g}^{-1}$ ) above 0.9 V is attributed to surface reaction of the electrode with the electrolyte [22–24]. The flat plateau at 0.8 V in the range of  $0.2 < x < 1.5$  observed in the charge curve signifies the co-existence of multiphases during which the  $\text{Co}_2\text{MnSi}$  electrode is converted into a lithiated form. A similar plateau has also been observed during the first charge cycle for  $\text{CoMnSb}$  with a half-Heusler structure. It was shown that at the plateau  $\text{CoMnSb}$  transformed to the full-Heusler type  $\text{Li}_2\text{CoSb}$  [23]. It is conjectured that a similar transformation also occurs for the  $\text{Co}_2\text{MnSi}$  electrode; this will be substantiated later.

Although 3.9 moles of Li are inserted into  $\text{Co}_2\text{MnSi}$  during the first charge, only 1.4 moles are extracted in the first discharge, which corresponds to the first irreversible capacity of  $320 \text{ mAh g}^{-1}$ . The exceedingly large irreversible capacity during the first cycle is believed to be related to the intrinsic structural change incurred during charging. Both  $\text{Cu}_2\text{Sb}$  and  $\text{CoMnSb}$ , which transform to  $\text{Li}_2\text{CoSb}$  with a full-Heusler type structure, have been found to exhibit a large irreversible capacity loss during the first cycle [22–24]. After the first cycle, however, the  $\text{Co}_2\text{MnSi}$  electrode gives reasonably steady cycling, as can be seen from subsequent charge–discharge curves. When the electrode is subjected

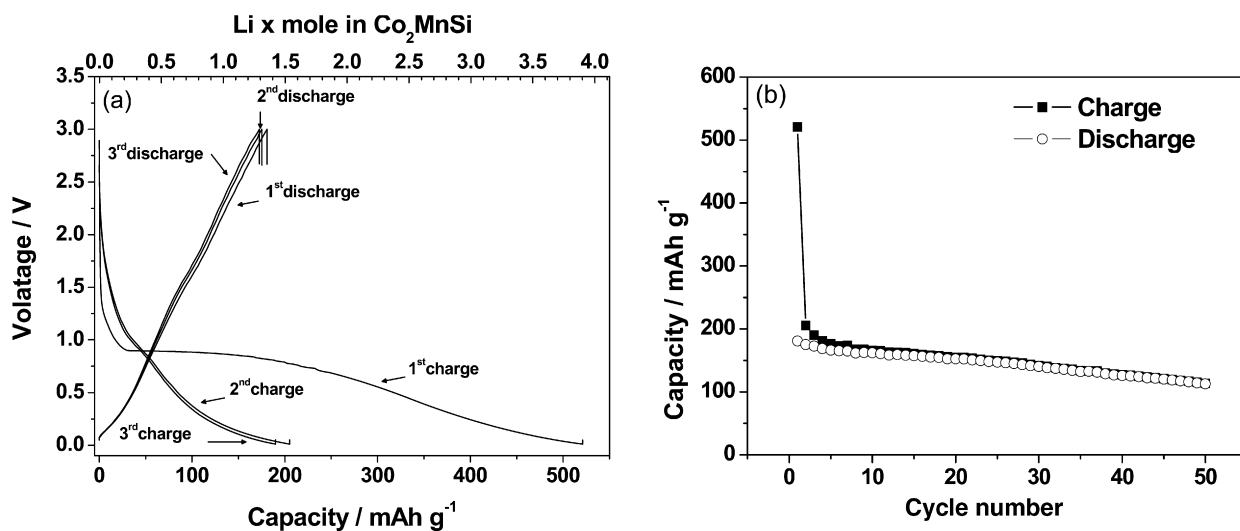


Fig. 1. (a) Charge–discharge curves of  $\text{Li}/\text{Co}_2\text{MnSi}$  cell cycled between 0.01 and 3 V at  $0.2 \text{ mA cm}^{-2}$  and (b) cycle performance of  $\text{Co}_2\text{MnSi}$  electrode.

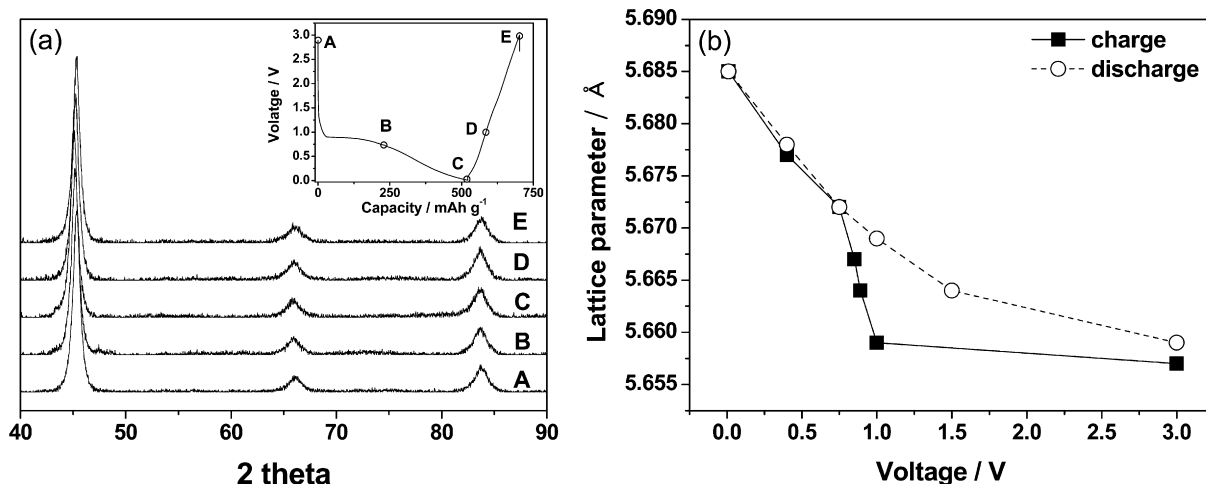


Fig. 2. (a) Evolution of ex situ XRD patterns for  $\text{Co}_2\text{MnSi}$  electrode during first charging and discharging. Inset: Voltage profile for first charge–discharge of  $\text{Li}/\text{Co}_2\text{MnSi}$  cell. Voltages at which XRD patterns were recorded are indicated by letters (A)–(E) in voltage profile: (A) as prepared; (B) 0.75 V; (C) 0.01 V (during charge) and (D) 1 V; (E) 3 V during discharge and (b) change in lattice parameter during first charging and discharging cycle.

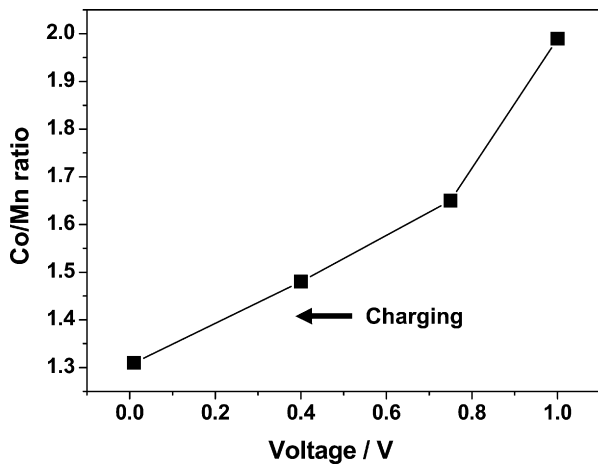


Fig. 3. Average Co:Mn ratio of individual Co<sub>2</sub>MnSi particles obtained with EDS at different states-of-charge during first charge.

to over 50 cycles, the discharge capacity slowly drops from 180 to 112 mAh g<sup>-1</sup> as is seen in Fig. 1(b).

A series of ex situ XRD data taken at different states-of-charge during the first cycle is shown in Fig. 2(a). In contrast to the reaction suggested by the plateau at 0.9 V, all of the XRD patterns are indexed to a fcc structure. Hence, no change in crystal structure is observed during the charge–discharge cycle, except for a change in the lattice parameter. The lattice parameter of the electrode as a function of cell voltage is presented in Fig. 2(b). During the charge, there is a sharp increase in the lattice volume between 1 and 0.75 V that corresponds to the flat plateau observed at 0.9 V during the charge cycle (Fig. 1(a)). The abrupt lattice expansion suggests a first-order phase transformation, associated with Co<sub>2</sub>MnSi transforming to Li<sub>2</sub>MnSi.

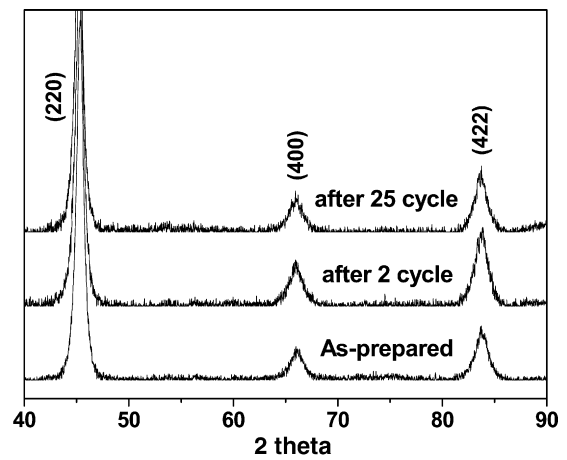


Fig. 4. XRD patterns of cycled Co<sub>2</sub>MnSi electrodes.

A change in the crystal structure is not observed because Co<sub>2</sub>MnSi and Li<sub>2</sub>MnSi possess identical crystal structures. Hence, the following reaction mechanism is proposed for the plateau in the charge cycle:



Beyond 0.75 V, the lattice volume further expands without any discontinuity. During the discharge cycle, the lattice volume also contracts without any abrupt changes and thereby indicates that the transition from Co<sub>2</sub>MnSi to Li<sub>2</sub>MnSi is irreversible. This suggests that after the transformation, Li insertion and removal proceeds by forming a solid solution. The proposed overall reaction can be described with reaction (1) occurring in the first charge cycle and

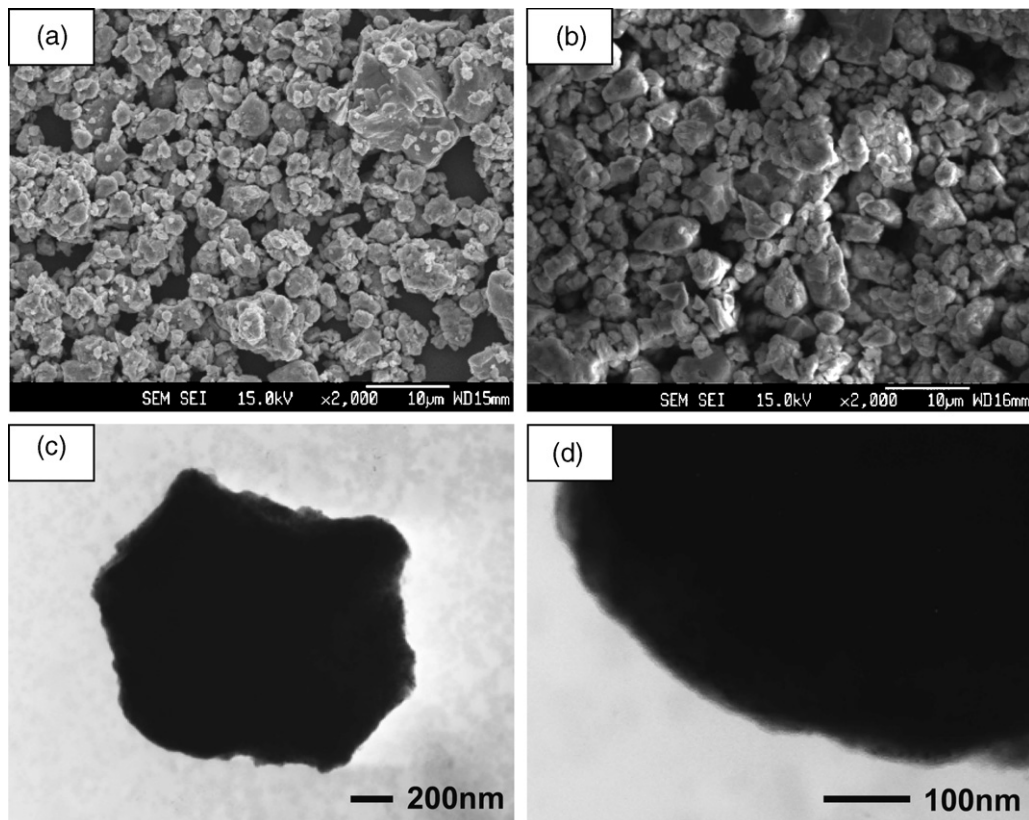
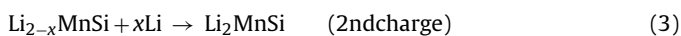
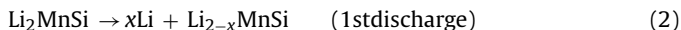


Fig. 5. SEM images of Co<sub>2</sub>MnSi powder: (a) before cycling, (b) after 25 cycles, (c) TEM bright-field image of Co<sub>2</sub>MnSi particle after 25 cycles and (d) magnified image of (c).

then followed by:



To substantiate further the suggested reaction (1), transmission electron microscopy (TEM) samples were prepared from electrodes at different states-of-charge during the 1st charge. Local chemical compositions from individual particles were measured using EDS. Fig. 3 plots the average Co:Mn ratio obtained at different states-of-charge. The data show that the  $\text{Co}_2\text{MnSi}$  electrode becomes increasingly depleted in Co as Li is inserted into the electrode. The Co:Mn ratio is initially at 2.0, but systematically decreases during the first Li-insertion. As suggested by reaction (1), the compositional analysis strongly suggests that Co is extracted and replaced by Li. The substantial amount of Co remaining in the electrode after full charging also suggests that Li may enter the interstitial sites and therefore give rise to large irreversible capacity loss observed in the 1st cycle.

X-ray diffraction data obtained from the cycled  $\text{Co}_2\text{MnSi}$  electrodes after 2 and 25 cycles are presented in Fig. 4 together with those from the as-prepared material. The lattice parameter was  $a = 5.657 \text{ \AA}$  in the as-prepared state. No noticeable structural transition was observed after 2 cycles as well as after 25 cycles, although the lattice parameter gradually increases to  $5.669 \text{ \AA}$  after 25 cycles. The lattice expansion probably stems from the lithium atoms retained in the lattice. Although a gradual increase in the lattice volume is observed after repeated cycling, the crystal structure is basically well maintained. Scanning electron microscopy images in Fig. 5(a) and (b) compare the morphology of the  $\text{Co}_2\text{MnSi}$  particle

before and after 25 cycles. There are no visible changes in particle size after cycling in agreement with the XRD data (evidenced by no appreciable changes in peak width). Nor does the particle morphology significantly change after cycling. Low and magnified TEM bright-field images shown in Fig. 5(c) and (d) indicate that the particle surface remains smooth without any extensive damage after cycling. Extensive TEM observation of the particles shows no evidence for any other secondary phases such as Mn- or Co-oxides on the particle surface.

Magnetic measurements provide further confirmation of the proposed reactions. A series of magnetic hysteresis loops was measured at different states-of-charge. Fig. 6(a) compares the magnetic hysteresis loop of the fully charged electrode with the as-prepared material. The curves show that the fully lithiated phase remains ferromagnetic, but with slightly decreased saturation magnetization as indicated by the arrows. The fact that the electrode remained ferromagnetic after incorporation of Li suggests that Li atoms replace Co atoms in the  $\text{Co}_2\text{MnSi}$  lattice. Displacement of Mn atoms by Li should dramatically reduce the magnetic moment of the material because it is the Mn atoms that provide the strong magnetic moment to the Heusler structure (atomic magnetic moment for Co =  $1.3\mu_B$  and for Mn =  $3.5\mu_B$  in  $\text{Co}_2\text{MnSi}$  [25]). In fact, no reported ferromagnetic Heusler alloys contain Co atoms at the 4b site of the unit cell [25,26]. It is likely that  $\text{Li}_2\text{CoSi}$  would be a paramagnetic material at room temperature. Therefore, if the lithiated phase were  $\text{Li}_2\text{CoSi}$ , the ferromagnetic hysteresis loop in Fig. 6(a) should not be observed. The proposed reaction is, however, different from that hypothesized for  $\text{CoMnSb}$ , in which it was suggested that  $\text{Li}_2\text{CoSb}$  was the more likely form through Li occupation of Mn sites based on the formation energy calculation.

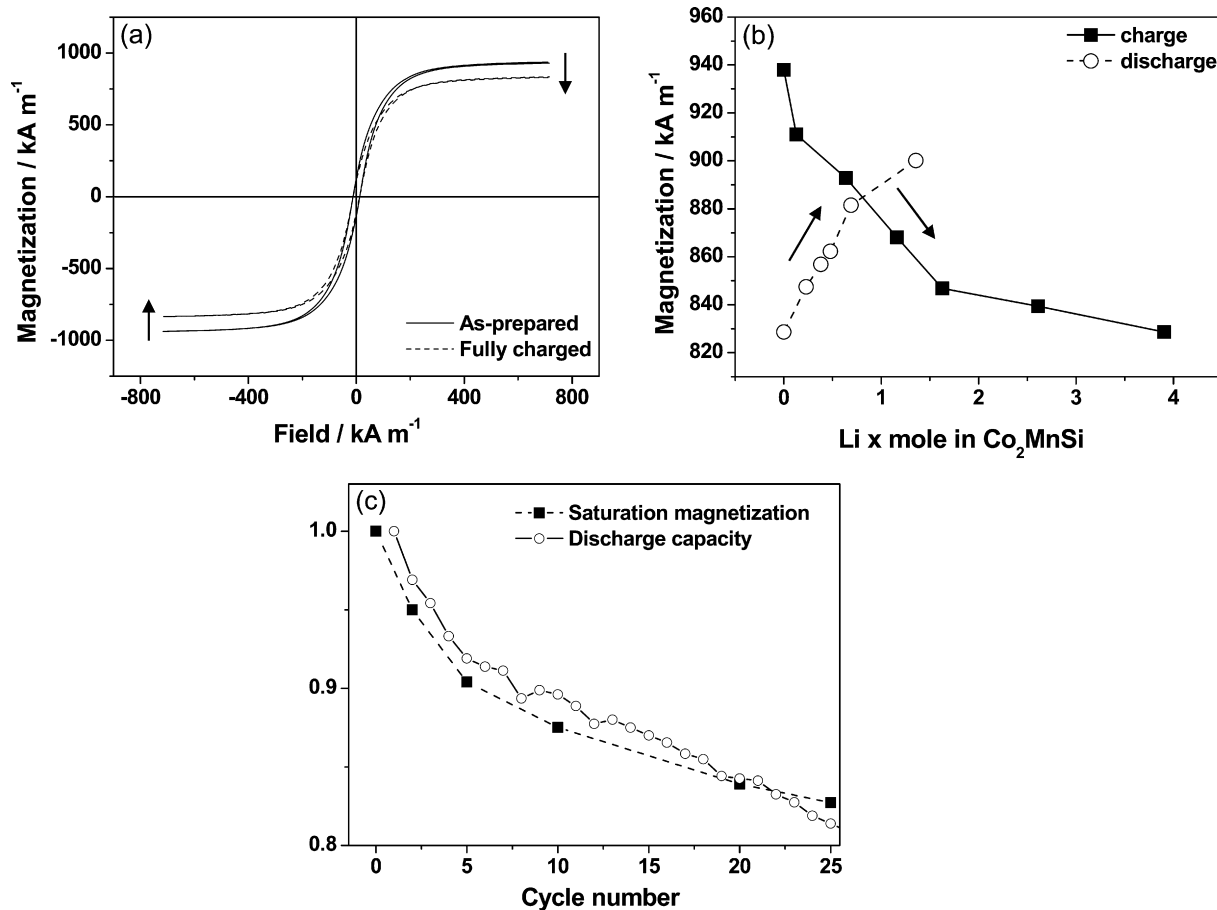


Fig. 6. (a) Magnetic hysteresis loops for as-prepared and fully charged  $\text{Co}_2\text{MnSi}$  electrode (first cycle), (b) saturation magnetization of  $\text{Co}_2\text{MnSi}$  electrode as function of state-of-charge during first cycle and (c) normalized plots of saturation magnetization of cycled electrodes and discharge capacity against cycle number.

Similar to the lattice parameter curve in Fig. 2(b), there is an abrupt change in the saturation magnetization during charging between 1.0 and 0.75 V, as can be seen from Fig. 6(b). The sharp drop in the saturation magnetization suggests that the electrode undergoes a phase transformation during the first Li insertion cycle. As the electrode is discharged, the removal of Li continuously raises the saturation magnetization without any abrupt changes. Thus, the behaviour of the magnetic properties is consistent with the proposed reaction. Fig. 6(b) shows the saturation magnetization as a function of the state-of-the-charge during the first cycle. The saturation magnetization progressively falls during Li charging as expected and then rises during removal of Li from the electrode. Note that the saturation magnetization does not attain the initial value of the as-prepared  $\text{Co}_2\text{MnSi}$ . The drop in the saturation magnetization after the first full cycle suggests that the chemical make-up of the electrode is fundamentally altered during cycling despite there being no changes in the crystal structure. Replacement of Co atoms with Li atoms would allow ferromagnetism but with a lower magnetic moment because Co atoms, which possess a relatively weak magnetic moment in  $\text{Co}_2\text{MnSi}$ , are removed from the unit cell. Hence, the magnetic measurements well support the proposed initial reaction that converts  $\text{Co}_2\text{MnSi}$  to  $\text{Li}_2\text{MnSi}$ .

Magnetic measurements were also performed on cycled electrodes; the normalized saturation magnetization of the cycled electrode is plotted against the number of cycles in Fig. 6(c). The saturation magnetization of the cycled electrode progressively decreases as cycling proceeds. The rate at which the saturation magnetization decreases is remarkably similar to the discharge capacity loss observed in Fig. 1(b). As can be seen in Fig. 6(c), the normalized curves for the saturation magnetization and the discharge capacity nearly coincide. This suggests the capacity loss is closely related to the change in the magnetic properties of the electrode. Increasing the fraction of non-magnetic Li retained in the lattice gradually reduces the saturation magnetization of the electrode. This reduction is also consistent with the XRD data in Fig. 4. Magnetic measurements are in agreement with the structural data and indicate that the reaction of  $\text{Co}_2\text{MnSi}$  with Li indeed proceeds in two steps and that retention of Li after each cycle is likely to be responsible for the slow deterioration of the discharge capacity.

#### 4. Conclusions

It is demonstrated that  $\text{Co}_2\text{MnSi}$  with a full-Heusler structure can be electrochemically cycled for Li-ion batteries. The compound exhibits a reversible discharge capacity of  $112 \text{ mAh g}^{-1}$  after 50 cycles. Based on structural analysis combined with magnetic properties, it is proposed that the reaction mechanism consists of two steps.  $\text{Co}_2\text{MnSi}$  transforms to Heusler-type  $\text{Li}_2\text{MnSi}$  during the first charge cycle and subsequent charge–discharge cycles involves

formation of a solid solution with  $\text{Li}_x\text{MnSi}$ . Further experiments to verify the proposed mechanism using different types of full-Heusler alloys are underway.  $\text{Co}_2\text{MnSi}$  may not be an ideal anode material for Li-ion batteries, but the intermetallic compound represents a class of materials that remain structurally robust during Li insertion/removal. In addition, because of the high density of the material compared with carbon anodes, appropriate chemical modification of the compound to increase the reversible discharge capacity would render its volumetric discharge capacity favourable compared with existing carbon-based anodes.

#### Acknowledgement

This work was supported by the research fund of Hanyang University (HY-2007-I).

#### References

- [1] M. Inaba, Z. Siroma, A. Funabiki, Z. Ogumi, *Langmuir* 12 (1996) 1534.
- [2] Y. Idota, T. Kubota, A. Matsufuji, Y. Maekawa, T. Miyasaka, *Science* 276 (1997) 1395.
- [3] M. Wachtler, J.O. Besenhard, M. Winter, *J. Power Sources* 94 (2001) 189.
- [4] H. Sakaguchi, H. Honda, Y. Akasaka, T. Esaka, *J. Power Sources* 119–121 (2003) 50.
- [5] J. Yin, M. Wada, S. Yoshida, K. Ishihara, S. Tanase, T. Sakai, *J. Electrochem. Soc.* 150 (2003) A1129.
- [6] J. Zhang, Y. Xia, *J. Electrochem. Soc.* 153 (2006) A1466.
- [7] H. Guo, H. Zhao, X. Jia, J. He, W. Qiu, X. Li, *J. Power Sources* 174 (2007) 921.
- [8] F. Wang, M. Zhao, X. Song, *J. Power Sources* 175 (2008) 558.
- [9] H. Kim, J. Choi, H.-J. Sohn, T. Kang, *J. Electrochem. Soc.* 146 (1999) 4401.
- [10] W.J. Weydanz, M. Wohlfahrt-Mehrens, R.A. Huggins, *J. Power Sources* 81–82 (1999) 237.
- [11] G.X. Wang, L. Sun, D.H. Bradhurst, S. Zhong, S.X. Dou, H.K. Liu, *J. Power Sources* 88 (2000) 278.
- [12] J. Wolfenstine, *J. Power Sources* 124 (2003) 241.
- [13] H. Dong, X.P. Ai, H.X. Yang, *Electrochem. Commun.* 5 (2003) 952.
- [14] I.-S. Kim, G.E. Blomgren, P.N. Kumta, *J. Power Sources* 130 (2004) 275.
- [15] D. Son, E. Kim, T. Kim, M. Kim, J. Cho, B. Park, *Appl. Phys. Lett.* 85 (2004) 5875.
- [16] M. Noh, Y. Kim, M.G. Kim, H. Lee, H. Kim, Y. Kwon, Y. Lee, J. Cho, *Chem. Mater.* 17 (2005) 3320.
- [17] G. Armstrong, A.R. Armstrong, P.G. Bruce, P. Reale, B. Scrosati, *Adv. Mater.* 18 (2006) 2597.
- [18] C.K. Chan, H. Peng, G. Liu, K. McIlwrath, X.F. Zhang, R.A. Huggins, Y. Cui, *Nature Nanotechnol.* 3 (2008) 31.
- [19] P. Poizot, S. Laruelle, S. Grugeon, L. Dupont, J.-M. Tarascon, *Nature* 407 (2000) 496.
- [20] J.-S. Do, C.-H. Weng, *J. Power Sources* 146 (2005) 482.
- [21] S.W. Oh, H.J. Bang, Y.C. Bae, Y.K. Sun, *J. Power Sources* 173 (2007) 502.
- [22] S. Matsuno, M. Noji, T. Kashiwagi, M. NaKayama, M. Wakihara, *J. Phys. Chem. C* 111 (2007) 7548.
- [23] S. Matsuno, M. NaKayama, M. Wakihara, *J. Electrochem. Soc.* 155 (2008) A61.
- [24] L.M.L. Fransson, J.T. Vaughey, R. Benedek, K. Edström, J.O. Thomas, *Electrochem. Commun.* 3 (2001) 317.
- [25] P.J. Brown, K.U. Neumann, P.J. Webster, K.R.A. Ziebeck, *J. Phys.: Condens. Matter* 12 (2000) 1827.
- [26] R. Poerschke, H.P.J. Wijn, *Data in Science and Technology Magnetic Properties of Metal*, Springer-Verlag, Berlin Heidelberg, Germany, 1991 (Ch. 7).